JACS
JOURNAL OF THE AMERICAN CHEMICAL SOCIETY
Communication
pubs.acs.org/JACS

3D Porous Crystalline Polyimide Covalent Organic Frameworks for Drug Delivery

Qianrong Fang,[†,‡] Junhua Wang,[‡] Shuang Gu,[‡] Robert B. Kaspar,[‡] Zhongbin Zhuang,[‡] Jie Zheng,[‡] Hongxia Guo,[‡,§] Shilun Qiu,*[,†] and Yushan Yan*[,‡]

[†]State Key Laboratory of Inorganic Synthesis and Preparative Chemistry, Jilin University, Changchun 130012, P. R. China

[‡]Department of Chemical and Biomolecular Engineering, Center for Catalytic Science and Technology, University of Delaware, Newark, Delaware 19716, United States

[§]College of Material Science and Engineering, Beijing University of Technology, Beijing 100124, P. R. China

Supporting Information

ABSTRACT: Three-dimensional porous crystalline polyimide covalent organic frameworks (termed PI-COFs) have been synthesized. These PI-COFs feature non- or interpenetrated structures that can be obtained by choosing tetrahedral building units of different sizes. Both PI-COFs show high thermal stability (>450 °C) and surface area (up to 2403 $m^2 g^{-1}$). They also show high loading and good release control for drug delivery applications.

Covalent organic frameworks (COFs),[1−4] an emerging class of porous crystalline polymers, have attracted attention for potential applications in gas storage and separation,[5,6] electronic devices,[7,8] energy storage,[9] temperature sensing,[10] and heterogeneous catalysis.[11,12] COFs are composed of light elements, typically H, B, C, N, and O, that crystallize into polymeric networks with highly ordered internal structures held together by strong covalent bonds. Since the pioneering work of Yaghi in 2005,[1] a variety of COFs have been reported. However, these COFs have been prepared through only a few chemical reactions, such as boronic acid trimerization,[13,14] boronate ester formation,[15,16] Schiff base reaction,[17,18] nitrile trimerization,[19,20] and nitroso self-addition,[21] limiting the possible structures and properties that can be achieved. Pore dimensionality is another limitation of the COF syntheses. While many two-dimensional (2D) COFs with layered eclipsed structures have been made available, the design, synthesis, and structural solution of three-dimensional (3D) COFs are still considered a challenge.

In this study, two new 3D polyimide COFs with high thermal stability and surface area, termed PI-COF-4 and PI-COF-5, were designed and synthesized by combining tetrahedral and linear building units via the imidization reaction. Interestingly, these two 3D PI-COFs feature non- or interpenetrated structures that can be obtained by choosing tetrahedral building units of different sizes. Furthermore, both PI-COFs exhibited high drug loading and well-controlled release profiles in drug delivery tests. To the best of our knowledge, this study is the first example of applying COF materials to drug delivery.

Our strategy for preparing the 3D porous PI-COFs is based on a diamond network with tetrahedral vertices. Through imidization, the linear linking unit, pyromellitic dianhydride (PMDA) (Scheme 1a), reacts with the tetrahedral building blocks 1,3,5,7-tetraaminoadamantane (TAA) (Scheme 1b) and tetra(4-aminophenyl)methane (TAPM) (Scheme 1c) to produce the extended 3D framework structures PI-COF-4 (Scheme 1d) and PI-COF-5 (Scheme 1e), respectively. Dehydration of the tetrahedral amines and the dianhydride yields linear bisimides, which assemble the tetrahedral building blocks into large structures with the diamond topology.[22] When such tetrahedral centers are separated by long rodlike links, the resulting structures tend to be interpenetrated.[23] In light of the different sizes of TAA and TAPM (3.1 and 5.9 Å; Figure S1 in the Supporting Information) and their formative bisimide links (13.0 and 18.6 Å; Figure S2), non- and multiply interpenetrated diamond nets were expected and indeed observed here for PI-COF-4 and -5, respectively (Scheme 1f,g).

Typically, syntheses were carried out by suspending PMDA (43.6 mg, 0.2 mmol) and TAA (19.6 mg, 0.1 mmol) or TAPM (38.1 mg, 0.1 mmol) in a mixture of *N*-methyl-2-pyrrolidone (NMP) (0.2 mL), mesitylene (1.0 mL), and isoquinoline (0.02 mL) followed by heating at 160 °C for 5 days, giving crystalline solids in yields of 86% for PI-COF-4 and 81% for PI-COF-5. These products are insoluble in water and common organic solvents such as acetone, ethanol, hexanes, tetrahydrofuran, *N*,*N*-dimethylformamide, and *m*-cresol.

Scanning electron microscopy (SEM) images show that both PI-COFs crystallized with a uniform rectangular morphology (Figures S3 and S4). In the Fourier transform infrared (FT-IR) spectra (Figures S5 and S6), absorptions at 1774 and 1718 cm^{-1} for PI-COF-4 and 1778 and 1720 cm^{-1} for PI-COF-5 are assigned to asymmetric and symmetric stretching vibrations, respectively, of C═O groups of the five-membered imide rings, whereas peaks at 1336 cm^{-1} for PI-COF-4 and 1353 cm^{-1} for PI-COF-5 are attributed to the stretching vibration of the C−N−C moieties. No bands corresponding to the starting monomers (amine around 3300 cm^{-1} and anhydride at 1765 cm^{-1}) or amic acid intermediates (amide around 1650 cm^{-1}) appeared, demonstrating that the products are fully imidized networks. Solid-state ^{13}C cross-polarization/magic-angle-spinning (CP/MAS) NMR spectra (Figure S7) confirmed the

Received: April 21, 2015
Published: June 22, 2015

DOI: 10.1021/jacs.5b04147
J. Am. Chem. Soc. 2015, 137, 8352−8355

Scheme 1. Strategy for Preparing 3D Porous Crystalline Polyimide COFs (PI-COFs)[a]

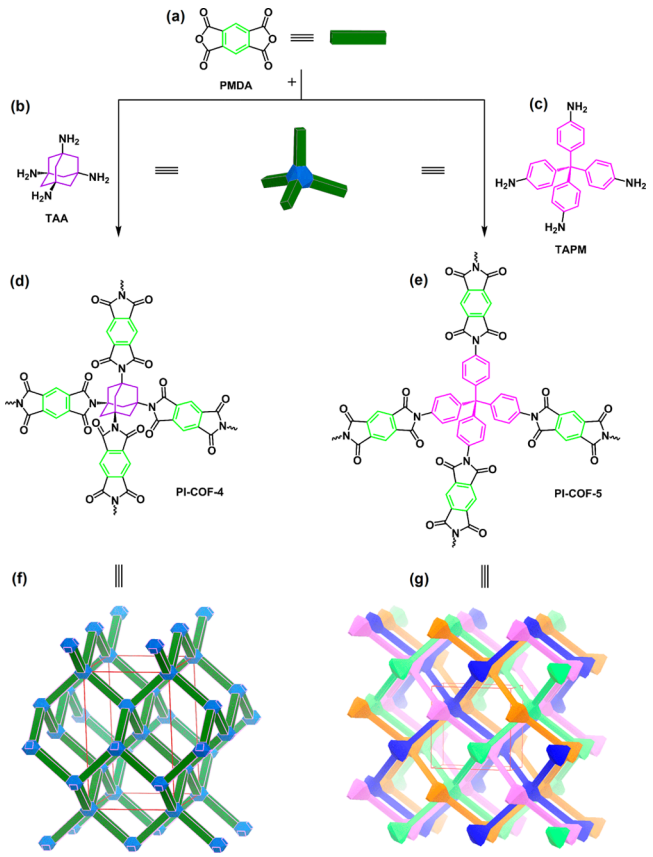

[a]Condensation of pyromellitic dianhydride (PMDA) (a) and tetrahedral 1,3,5,7-tetraaminoadamantane (TAA) (b) or tetra(4-aminophenyl)methane (TAPM) (c) gives PI-COF-4 (d) or PI-COF-5 (e). Linking of the linear and tunable tetrahedral building units affords the products with 3D structures based on non-interpenetrated (f) or interpenetrated (g) diamond nets.

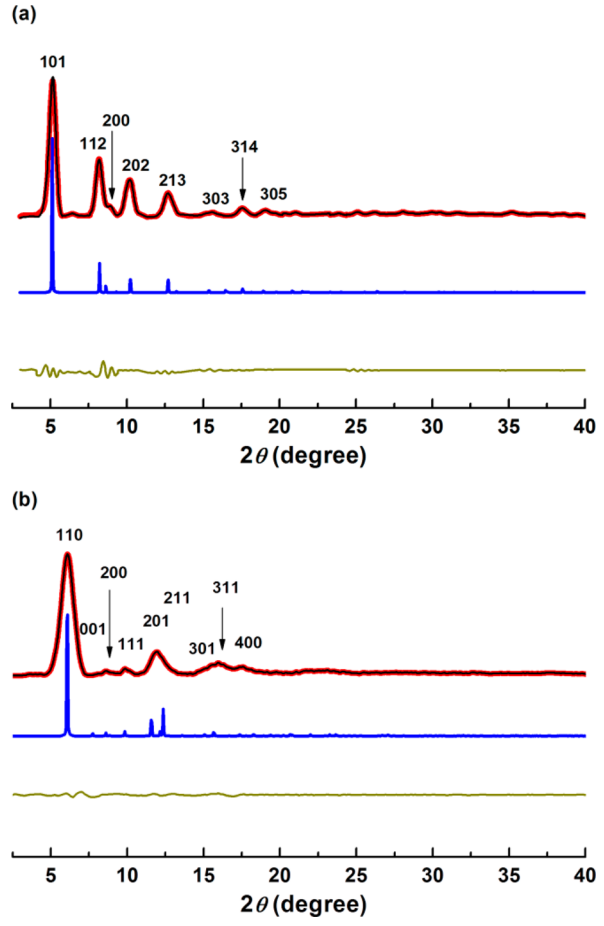

Figure 1. PXRD patterns of (a) PI-COF-4 and (b) PI-COF-5 with the observed profiles in black, refined in red, calculated in blue, and the difference (observed minus refined) in dark yellow.

carbonyl carbon from the imide ring at 165 ppm for PI-COF-4 and 164 ppm for PI-COF-5. The carbonyl signal of the amic acid group at around 176 ppm did not appear. Both PI-COFs exhibited high thermal stability in thermogravimetric analysis (TGA): up to 450 °C for PI-COF-4 and 460 °C for PI-COF-5 (Figures S8 and S9). In order to explore the polyimide formation, FT-IR spectroscopy and powder X-ray diffraction (PXRD) were performed at different times (Figures S10−S13). The FT-IR spectra after 1, 3, and 5 days were similar, and the characteristic absorption bands of the amic acid intermediate could not be observed. In contrast, PXRD patterns showed no crystalline phase for the sample at 1 day and very weak peaks for the sample at 3 days, whereas after 5 days the PI-COF products with good crystallinity were confirmed by their PXRD patterns. These results suggested that once the amine and anhydride react to yield the amic acid intermediate, the subsequent imide ring-closing reactions are completed under these synthetic conditions. In addition, these observations implied that the formation of crystalline PI-COFs is slow and that it takes some time to adjust their positions to obtain the crystalline phase by the reversible reaction, which is consistent with the covalent-bond-forming reactions of other COFs.[1−4]

The crystallinities and unit cell parameters of both PI-COFs were determined by PXRD analysis (Figure 1). After a geometrical energy minimization based on the non- or fourfold-interpenetrated diamond net for PI-COF-4 and PI-COF-5, respectively, the unit cell parameters were obtained ($a = b = 20.49$ Å, $c = 32.20$ Å, $\alpha = \beta = \gamma = 90°$ for PI-COF-4; $a = b = 20.57$ Å, $c = 11.43$ Å, $\alpha = \beta = \gamma = 90°$ for PI-COF-5). The simulated PXRD patterns were in excellent agreement with the experimental ones (Figure 1, black and blue curves, respectively). Furthermore, full profile pattern matching (Pawley) refinements were carried out on the experimental PXRD patterns. Peaks at 5.12, 8.20, 8.62, 10.22, 12.70, 15.36, 17.56, and 18.94° for PI-COF-4 correspond to the (101), (112), (200), (202), (213), (303), (314), and (305) Bragg peaks of space group $P4_1/amd$ (No. 141), respectively, and peaks at 6.10, 7.75, 8.60, 9.85, 11.55, 12.35, 15.05, 15.65, and 17.40° for PI-COF-5 correspond to the (110), (001), (200), (111), (201), (211), (301), (311), and (400) Bragg peaks of space group $P4/n$ (No. 85), respectively. The refinement results yield unit cell parameters nearly equivalent to the predictions with good agreement factors ($a = b = 20.41$ Å, $c = 32.16$ Å, $\alpha = \beta = \gamma = 90°$, $wR_p = 7.95\%$, $R_p = 4.58\%$ for PI-COF-4; $a = b = 20.63$ Å, $c = 11.50$ Å, $\alpha = \beta = \gamma = 90°$, $wR_p = 9.62\%$, $R_p = 6.83\%$ for PI-COF-5). We also considered alternative structures for both PI-COFs. Two- and threefold-interpenetrated diamond nets for PI-COF-4 were constructed from the space groups $P4_2/n$ (No. 86) and $I4_1/amd$, respectively, and non-, twofold-, and threefold-interpenetrated diamond nets were constructed for PI-COF-5 from space

DOI: 10.1021/jacs.5b04147
J. Am. Chem. Soc. 2015, 137, 8352−8355

groups $I4_1/amd$, $P4_2/n$, and $I4_1/amd$, respectively. However, the simulated PXRD patterns from these alternative nets did not match the experimental data (Figures S14−S22 and Tables S1−S7).

On the basis of the above results, both PI-COFs are proposed to have the expected architectures with non- and fourfold-interpenetrated diamond nets (Figure 2). For PI-COF-4, a single diamond net is constructed from 10 TAA and 12 PMDA molecules (Figure 2a,b) with a cage size of 17 Å, and these diamond nets are further connected by PMDA linkers to form a 3D non-interpenetrated open framework with an aperture size of about 15 Å running along the *a* or *b* axis (Figure 2c). For PI-COF-5, the single diamond net assembled from 10 TAPM and 12 PMDA molecules has a larger 28 Å cage (Figure 2d), which allows for fourfold interpenetration along the *c* axis (Figure 2e). The overall structure has 1D rectangular channels that are about 11 Å in width running along the *c* axis (Figure 2f).

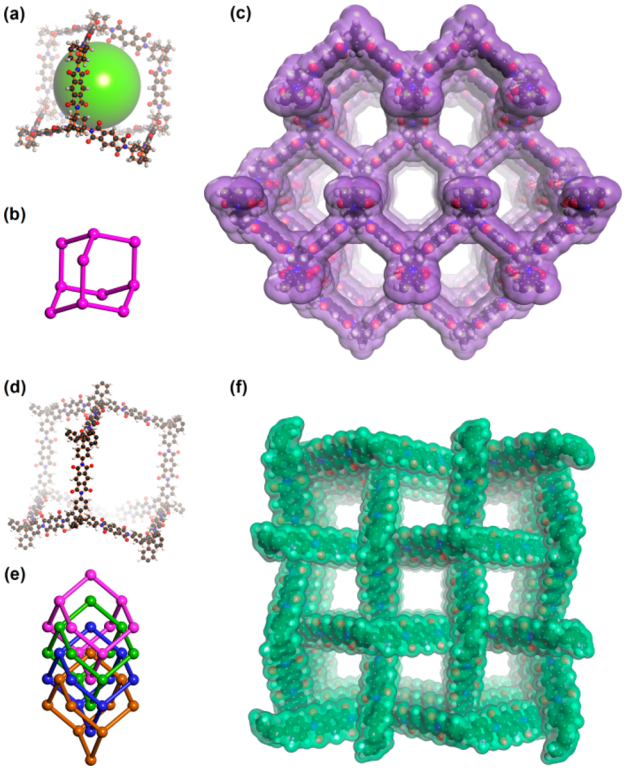

Figure 2. Structural representations of 3D PI-COFs. (a−c) Extended structure of PI-COF-4: (a) single diamond network; (b) diamond topology; (c) 3D porous structure with 15 Å pores. (d−f) Extended structure of PI-COF-5: (d) single diamond network; (e) fourfold-interpenetrated diamond topology; (f) 3D structure with 11 Å pores. C, black; H, gray; N, blue; O, red.

The permanent porosities of the PI-COFs were determined by measuring N_2 adsorption at 77 K. Both exhibit classic type-I isotherms characterized by a sharp uptake under low relative pressures in the range of $P/P_0 = 10^{-5}$−10^{-2} (Figure 3), a signature feature of microporous materials. The lack of hysteresis indicates that the adsorption and desorption mechanisms are similar and that the adsorption is reversible. The Brunauer−Emmett−Teller (BET) surface areas were found to be 2403 $m^2\ g^{-1}$ for PI-COF-4 and 1876 $m^2\ g^{-1}$ for PI-COF-5 (Figures S23 and S24). The pore-size distributions

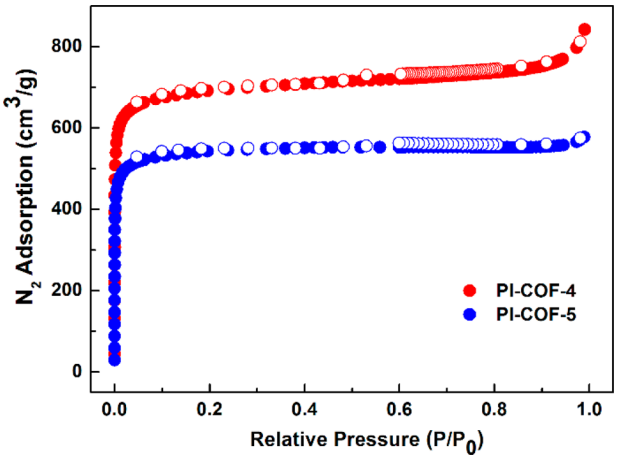

Figure 3. N_2 adsorption isotherms for the 3D PI-COFs at 77 K. Solid and open circles represent adsorption and desorption branches, respectively.

of the PI-COFs were calculated by nonlocal density functional theory. Both PI-COFs show narrow pore widths (13 Å for PI-COF-4 and 10 Å for PI-COF-5; Figures S25 and S26), in agreement with the theoretical values predicted from their crystal structures (15 and 11 Å, respectively).

Encouraged by their large pores and high surface area, we employed these 3D PI-COFs to control drug delivery in vitro. Ibuprofen (IBU) was chosen as a model drug because the pore size of the PI-COFs is large enough for "comfortable" entrapment of IBU (molecular size 5 Å × 10 Å).[24] IBU is well-known as a nonsteroidal anti-inflammatory drug and is widely used to treat inflammation, pain, and rheumatism. However, the drug has a short biological half-life (2 h),[25] which makes it a candidate for sustained or controlled drug delivery. Therefore, IBU has been employed frequently as a model drug to study sustained/controlled release. Recent reports have demonstrated that mesoporous silica materials[26] or metal−organic frameworks[27] can serve as drug carriers. COFs have large pores and excellent stability and thus are expected to be effective materials for drug delivery. However, COFs have not been explored for drug delivery applications.

Typically, to load the drug, the PI-COFs were immersed in IBU hexane solution, stirred for 2 h, filtered, and washed. The resultant PXRD peaks and SEM images coincide with those of the starting material, confirming the structural integrity after loading (Figures S27−S30). Because of the presence of the drug in the pores, the nitrogen adsorption isotherms of the IBU-loaded PI-COFs at 77 K indicate a decrease in specific surface area (to 1085 $m^2\ g^{-1}$ for PICOF-4 and 699 $m^2\ g^{-1}$ for PICOF-5; Figures S31−S34). Furthermore, IBU was evaluated in IBU-loaded PI-COF-4 and PI-COF-5 at concentrations of 24 and 20 wt %, respectively, based on TGA (Figures S35−S37). The drug release profiles were detected by UV−vis spectrophotometry using a calibration curve for IBU (Figure 4). Compared with PI-COF-4, PI-COF-5 with the smaller pore size and interpenetrated structure shows a lower release rate (e.g., 60% for PI-COF-4 vs 49% for PI-COF-5 after 12 h), which reveals that the drug delivery in COFs is directly related to the pore size and geometry. For both PI-COFs, the majority of the IBU was released after about 6 days, and total delivery could reach ca. 95% of the initial IBU loading. To further investigate the application of COFs in drug delivery, two other drug molecules, captopril[28] for the treatment of hypertension

DOI: 10.1021/jacs.5b04147
J. Am. Chem. Soc. 2015, 137, 8352−8355

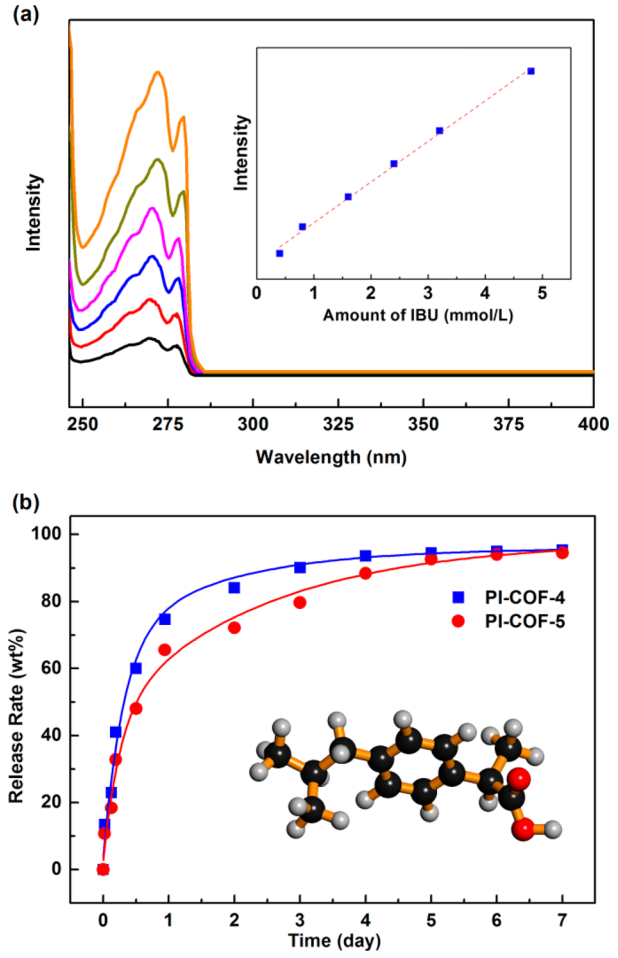

Figure 4. (a) UV−vis spectra of ibuprofen (IBU) in simulated body fluid (SBF) (pH 7.4, buffer solution) at different concentrations. Inset: IBU calibration curve. (b) Release profiles of IBU-loaded 3D PI-COFs. Inset: the structure of IBU. C, black; H, gray; O, red.

and congestive heart failure and caffeine[29] as a psychoactive drug, also were studied. The results showed that COFs loaded with these drugs have good release control, is similar to that of the IBU-loaded COFs (Figures S38 and S39 and Table S8).

In conclusion, we have for the first time synthesized two novel 3D porous PI-COFs with non- or fourfold-interpenetrated diamond networks via an imidization reaction. Both PI-COFs showed high thermal stability and surface area. They are the first COFs ever to be employed in controlled drug delivery, for which they show high loadings and good release control. These results should facilitate the development of COFs for pharmaceutical applications. Further studies are currently underway in our laboratory.

■ ASSOCIATED CONTENT

Supporting Information

Synthetic procedures and SEM, FTIR, solid-state ^{13}C NMR, TGA, PXRD, N_2 adsorption, BET, and pore size distribution results. The Supporting Information is available free of charge on the ACS Publications website at DOI: 10.1021/jacs.5b04147.

■ AUTHOR INFORMATION

Corresponding Authors

*sqiu@jlu.edu.cn

*yanys@udel.edu

Notes

The authors declare no competing financial interest.

■ ACKNOWLEDGMENTS

This work was supported by the University of Delaware, the National Natural Science Foundation of China (91022030), the National Basic Research Program of China (2011CB808703), and the "111" Project (B07016).

■ REFERENCES

(1) Côté, A. P.; Benin, A. I.; Ockwig, N. W.; O'Keeffe, M.; Matzger, A. J.; Yaghi, O. M. *Science* **2005**, *310*, 1166.
(2) Colson, J. W.; Woll, A. R.; Mukherjee, A.; Levendorf, M. P.; Spitler, E. L.; Shields, V. B.; Spencer, M. G.; Park, J.; Dichtel, W. R. *Science* **2011**, *332*, 228.
(3) Feng, X.; Ding, X.; Jiang, D. *Chem. Soc. Rev.* **2012**, *41*, 6010.
(4) Ding, S.-Y.; Wang, W. *Chem. Soc. Rev.* **2013**, *42*, 548.
(5) Furukawa, H.; Yaghi, O. M. *J. Am. Chem. Soc.* **2009**, *131*, 8875.
(6) Han, S. S.; Mendoza-Cortes, J. L.; Goddard, W. A., III. *Chem. Soc. Rev.* **2009**, *38*, 1460.
(7) Wan, S.; Guo, J.; Kim, J.; Ihee, H.; Jiang, D. *Angew. Chem., Int. Ed.* **2008**, *47*, 8826.
(8) Bertrand, G. H. V.; Michaelis, V. K.; Ong, T. C.; Griffin, R. G.; Dincă, M. *Proc. Natl. Acad. Sci. U.S.A.* **2013**, *110*, 4923.
(9) DeBlase, C. R.; Silberstein, K. E.; Thanh-Tam, T.; Abruna, H. D.; Dichtel, W. R. *J. Am. Chem. Soc.* **2013**, *135*, 16821.
(10) Fang, Q. R.; Zhuang, Z. B.; Gu, S.; Kaspar, R. B.; Zheng, J.; Wang, J. H.; Qiu, S. L.; Yan, Y. S. *Nat. Commun.* **2014**, *5*, No. 4503.
(11) Ding, S. Y.; Gao, J.; Wang, Q.; Zhang, Y.; Song, W. G.; Su, C. Y.; Wang, W. *J. Am. Chem. Soc.* **2011**, *133*, 19816.
(12) Fang, Q. R.; Gu, S.; Zheng, J.; Zhuang, Z. B.; Qiu, S. L.; Yan, Y. S. *Angew. Chem., Int. Ed.* **2014**, *53*, 2878.
(13) El-Kaderi, H. M.; Hunt, J. R.; Mendoza-Cortés, J. L.; Côté, A. P.; Taylor, R. E.; O'Keeffe, M.; Yaghi, O. M. *Science* **2007**, *316*, 268.
(14) Wan, S.; Guo, J.; Kim, J.; Ihee, H.; Jiang, D. *Angew. Chem., Int. Ed.* **2009**, *48*, 5439.
(15) Spitler, E. L.; Dichtel, W. R. *Nat. Chem.* **2010**, *2*, 672.
(16) Tilford, R. W.; Mugavero, S. J., III; Pellechia, P. J.; Lavigne, J. J. *Adv. Mater.* **2008**, *20*, 2741.
(17) Uribe-Romo, F. J.; Hunt, J. R.; Furukawa, H.; Klöck, C.; O'Keeffe, M.; Yaghi, O. M. *J. Am. Chem. Soc.* **2009**, *131*, 4570.
(18) Kandambeth, S.; Mallick, A.; Lukose, B.; Mane, M. V.; Heine, T.; Banerjee, R. *J. Am. Chem. Soc.* **2012**, *134*, 19524.
(19) Kuhn, P.; Antonietti, M.; Thomas, A. *Angew. Chem., Int. Ed.* **2008**, *47*, 3450.
(20) Bojdys, M. J.; Jeromenok, J.; Thomas, A.; Antonietti, M. *Adv. Mater.* **2010**, *22*, 2202.
(21) Beaudoin, D.; Maris, T.; Wuest, J. D. *Nat. Chem.* **2013**, *5*, 830.
(22) Bonneau, C.; Delgado-Friedrichs, O.; O'Keeffe, M.; Yaghi, O. M. *Acta Crystallogr.* **2004**, *A60*, 517.
(23) Zhang, Y. B.; Su, J.; Furukawa, H.; Yun, Y. F.; Gandara, F.; Duong, A.; Zou, X. D.; Yaghi, O. M. *J. Am. Chem. Soc.* **2013**, *135*, 16336.
(24) Vallet-Regi, M.; Rámila, A.; del Real, R. P.; Pérez-Pariente, J. *Chem. Mater.* **2001**, *13*, 308.
(25) Highton, F. The Pharmaceutics of Ibuprofen. In *Ibuprofen: A Critical Bibliographic Review*; Rainsford, K.D., Ed.; Taylor & Francis: London, 1999; p 53.
(26) Qu, F. Y.; Zhu, G. S.; Lin, H. M.; Zhang, W. W.; Sun, J. Y.; Li, S. G.; Qiu, S. L. *J. Solid State Chem.* **2006**, *179*, 2027.
(27) Horcajada, P.; Serre, C.; Vallet-Regí, M.; Sebban, M.; Taulelle, F.; Férey, G. *Angew. Chem., Int. Ed.* **2006**, *45*, 5974.
(28) Nur, A. O.; Zhang, J. S. *Int. J. Pharm.* **2000**, *66*, 139.
(29) Glade, M. J. *Nutrition* **2010**, *26*, 932.

DOI: 10.1021/jacs.5b04147
J. Am. Chem. Soc. 2015, 137, 8352−8355